Industrial emissions cause extreme urban ozone diurnal variability

Renyi Zhang*†, Wenfang Lei*, Xuexi Tie‡, and Peter Hess‡

*Department of Atmospheric Sciences, Texas A&M University, College Station, TX 77843; and ‡Atmospheric Chemistry Division, National Center for Atmospheric Research, Boulder, CO 80307

Communicated by Mario J. Molina, Massachusetts Institute of Technology, Cambridge, MA, March 10, 2004 (received for review November 11, 2003)

Simulations with a regional chemical transport model show that anthropogenic emissions of volatile organic compounds and nitrogen oxides (NO_x = NO + NO_2) lead to a dramatic diurnal variation of surface ozone (O_3) in Houston, Texas. During the daytime, photochemical oxidation of volatile organic compounds catalyzed by NO_x results in episodes of elevated ambient O_3 levels significantly exceeding the National Ambient Air Quality Standard. The O_3 production rate in Houston is significantly higher than those found in other cities over the United States. At night, a surface NO_x maximum occurs because of continuous NO emission from industrial sources, and, consequently, an extensive urban-scale "hole" of surface ozone (<10 parts per billion by volume in the entire Houston area) is formed as a result of O_3 removal by NO. The results suggest that consideration of regulatory control of O_3 precursor emissions from the industrial sources is essential to formulate ozone abatement strategies in this region.

Elevated levels of airborne pollutants have been a widespread environmental problem in urban and rural areas throughout the United States (1–5). In particular, Houston, Texas, has received considerable scientific and political attention because of its ozone nonattainment over the National Ambient Air Quality Standard (NAAQS) (5–7). In addition to being one of the largest metropolitan areas in the United States, Houston houses one of the world's largest petrochemical complexes and contains a concentrated network of large coal-fired power plants. Anthropogenic emissions of volatile organic compounds (VOCs) and nitrogen oxides (NO_x = NO + NO_2) lead to distinct chemical features in the atmosphere. Most noticeably, elevated ozone levels are produced as a result of photochemical oxidation of VOCs catalyzed by NO_x in the presence of sunlight (8–10). High concentrations of surface ozone have been shown to impose deleterious effects on human health and the ecosystem (11). Regulation of ozone precursor emissions under the United States Clean Air Act of 1970 and its subsequent amendments have been developed to reduce human exposure. Early ozone management strategies emphasized reduction of VOC and NO_x emissions from on- and off-road automobiles, and recent attention under the state implementation plan (SIP) has been focused on NO_x from electric utility power plants and VOCs and NO_x from petrochemical plants. Development and enforcement of SIP, however, have been often hindered because of inadequate scientific understanding of the causes of high-ozone episodes and have invoked legal disputes between the state environmental agency and the industry. Although several observational results on O_3 formation and budget issues in this region have been published, to date very few results attained by using scientifically oriented chemical transport models (CTMs) have been published in the refereed literature.

In this study, we simulated the spatial and temporal distributions of O_3 and its precursors in the Houston metropolitan area by employing a regional CTM. The relationship between the rapid production, daily peak, and diurnal variation of surface O_3 and the concurrence of high anthropogenic VOC and NO_x emissions in this region is assessed.

Methods

The CTM was modified from a regional chemical transport model developed at the National Center for Atmospheric Research (NCAR) (12, 13). The horizontal grid resolution of 12 × 12 km was used, and there were 38 layers in the vertical direction from the surface to 100 mbar (1 bar = 100 kPa) in a terrain-following coordinate system with 7 layers in the lowest 50-mbar altitudes. The chemistry in the CTM included treatment of standard gas-phase and heterogeneous chemistry (12, 13). The inorganic chemistry part is similar to the original NCAR model (12), and the organic part is based on the CB-4 mechanism used in the Comprehensive Air Quality Model with the extension Version 3.1 (CAMX V3.1) (14). The CB-4 mechanism was modified to represent both polluted and remote tropospheric atmosphere (13). The isoprene oxidation mechanism was updated to accommodate the recent advances (15, 16). The heterogeneous reactions of NO_x on black carbon aerosol (soot) (17, 18) and N_2O_5 on sulfate aerosol (19) were included in the model. The chemical initial and lateral boundary conditions were interpolated from Modeling OZone And Related chemical Tracers (MOZART V.2), a global CTM (20). The CTM was driven by the output circulation field from a meteorological model, the Penn State/NCAR Mesoscale Model, Version 5 (MM5) (21). The diurnally varied sea/land breeze dominates the circulation pattern in this region (22). Throughout the simulation episode, the meteorological fields obtained by MM5 well reproduced available observed daytime and nighttime surface wind and temperature fields and the planetary boundary layer structures (13).

A stagnant ozone pollution episode (September 7–11, 1993) was chosen for the model study. This period is selected because a strong diurnal variability of ozone occurred with the maximum concentration of larger than 200 parts per billion by volume (ppbv) during the day and the minimum concentration <10 ppbv during night. A surface emission inventory (EI) of chemically speciated (based on the CB-4 mechanism), spatially gridded (16 × 16 km), and temporally resolved (1-h averaged) was provided by the Texas Commission on Environmental Quality (TCEQ) (23, 24). Emissions beyond the TCEQ EI spatial coverage were interpolated from the MOZART input EI (1° × 1° resolution and daily averaged) (20). The industrial emission of olefins was adjusted according to recent field measurements from the 2000 Texas Air Quality Study (5). An extensive ground-based observation of O_3, NO_x, and other pollutants was conducted during the same time period associated with the Coastal Oxidant Assessment for Southern Texas (COAST) field project (23, 24). Industrial sources contribute significantly to the total VOC and NO_x emissions (Fig. 1). For example, the industrial emissions comprise ≈50% of the total NO_x over the Houston Metropolitan area and more in the industrial districts.

Abbreviations: CDT, central daylight time; CTM, chemical transport model; NO_x, NO + NO_2; ppbv, parts per billion by volume; VOC, volatile organic compound.

†To whom correspondence should be addressed at: Department of Atmospheric Sciences, Texas A&M University, 1204 Eller O&M Building, College Station, TX 77843. E-mail: zhang@ariel.met.tamu.edu.

www.pnas.org/cgi/doi/10.1073/pnas.0401484101

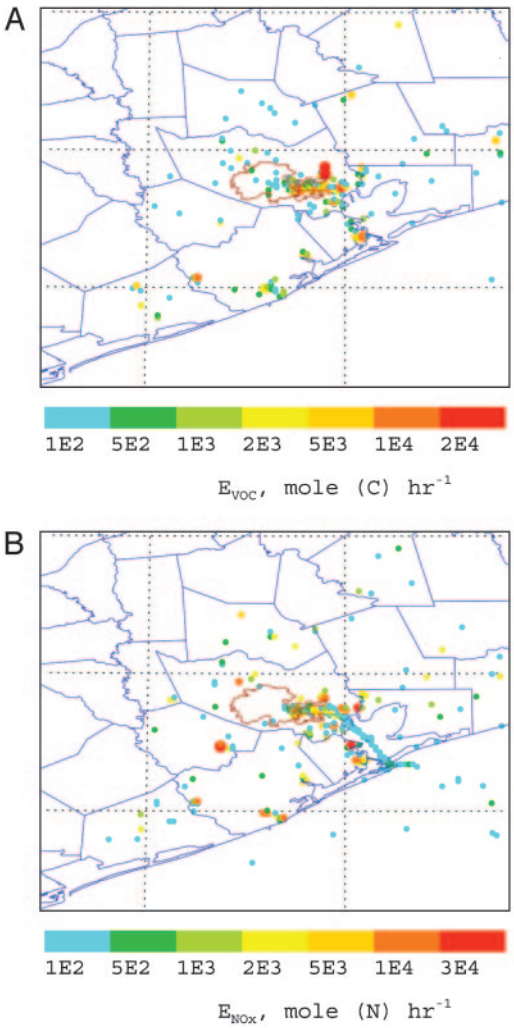

Fig. 1. Daily averaged industrial point emissions of VOCs (*A*) and NO_x (*B*) in the Houston metropolitan area during the model simulation period. The thin red lines mark the Houston City limit, and the blue lines label the county limits near Houston. In the NO_x panel, the blue dotted line along the Galveston Bay corresponds to ship emissions. The sizes of the symbols correlate to the emission strengths. The high emissions of VOCs and NO_x concentrating near the Houston Ship Channel and along the west coastline of the Galveston Bay are from petrochemical plants. Another intensive NO_x emission to the southwest of the Houston downtown area is from utility power plants. Diurnal variations of the industrial VOC and NO_x emissions are generally within 20%.

The high emissions of VOCs and NO_x concentrating near the Houston Ship Channel and along the west coastline of the Galveston Bay are from petrochemical plants. Another intensive NO_x emission to the southwest of the Houston downtown area is from utility power plants. Diurnal variations of the industrial VOC and NO_x emissions are generally within 20%.

Results and Discussion

The simulated spatial distributions of the daytime [3 p.m. central daylight time (CDT)] and nighttime (11 p.m. CDT) O_3 and NO_x in the lowest model layer (about 30 m above ground level) are depicted in Fig. 2. A maximal zone of daytime surface ozone with concentrations exceeding 125 ppbv is located to the southeast region of the Houston downtown area, extending from the Houston Ship Channel to the Galveston Bay (Fig. 2*B*). The occurrence of this zone coincides with the industrial corridor with high VOC and NO_x emissions from petrochemical plants (Fig. 1). During the daytime, photochemical oxidation of VOCs initiated by hydroxyl radicals OH produces organic peroxy radicals (RO_2), facilitating cycling of NO to NO_2 and formation of tropospheric ozone.

$$OH + VOC(+ O_2) \rightarrow RO_2 \quad [1]$$

$$RO_2 + NO \rightarrow RO + NO_2 \quad [2]$$

$$NO_2 + h\nu \rightarrow NO + O \quad [3]$$

$$O + O_2 \rightarrow O_3 \quad [4]$$

The model calculates a highest surface O_3 concentration of 212 ppbv at 3 p.m. located slightly southeast to the Houston Ship Channel, in agreement with the ground-based ozone observations showing that a 1-h averaged daily O_3 peak of 214 ppbv was measured during the same time period at a nearby monitoring site. A narrow O_3 deficit zone roughly along the west coastline of the Galveston Bay divides the maximal ozone region. This O_3 minimum may be explained because of NO_x emissions from petrochemical plants and ships on either side of this region (Fig. 1*B*). Because the daytime temperature over the ocean surface is relatively lower than that over the land surface, vertical mixing is rather insufficient over the ocean surface and along the coastline (13). NO_x emitted from this region is not efficiently transported vertically, resulting in the maximal NO_x zone (Fig. 2*D*). At high NO_x, the reaction $OH + NO_2 \rightarrow HNO_3$ becomes important, leading to removal of OH radicals and hence inhibiting photochemical O_3 formation.

In contrast to the daytime O_3 maximum, the model simulations show exceedingly low levels of nighttime surface ozone: an extensive O_3 hole covers much of the Houston metropolitan area (Fig. 2*A*) and persists throughout the night (i.e., from 8 p.m. to 6 a.m. CDT). It is evident that the surface O_3 hole correlates with a NO_x maximum (Fig. 2*C*). The elevated NO_x levels are attributed to continuous nighttime NO emissions from utility power plants located to the southwest of the downtown area and from petrochemical plants along the Houston Ship Channel and the Galveston Bay (Fig. 1). In addition, meteorological and chemical processes are also responsible for the nighttime NO_x maximum. During the night, the atmosphere is characterized by a more stability condition (no solar radiation) and hence inefficient vertical mixing, and NO_x emitted from industrial sources is trapped within the planetary boundary layer. Also, the photochemical process ceases at night, terminating chemical NO_x removal such as by the reaction of OH with NO_2 to form HNO_3 (23). Consequently, the large abundance of NO_x near the surface level leads to nearly complete removal of ozone by the reaction $NO + O_3 \rightarrow NO_2 + O_2$. We also assessed other plausible chemical and physical removal processes for the surface ozone. For example, ozone undergoes efficient dry deposition (25) and reacts with olefins (26, 27) that also are abundant because of emissions from petrochemical plants. Model sensitivity simulations reveal that those O_3 destruction and removal processes contribute negligibly to the nighttime O_3 loss in the Houston metropolitan area. In addition, we found that heterogeneous chemistry occurring on soot accounts for $<5\%$ of the nighttime NO_x removal.

The modeled diurnal variations of O_3 and NO_x over the Houston metropolitan area are displayed and compared to atmospheric observations in Fig. 3. The locations of the monitoring stations are marked as the brown dots in Fig. 2*C* (delimited within a brown rectangle which is referred as the Houston domain). The modeled values at the lowest model layer are linearly interpolated to a monitoring site from the four cells surrounding the monitoring station, and the comparisons are made for the O_3 and NO_x averaged over the

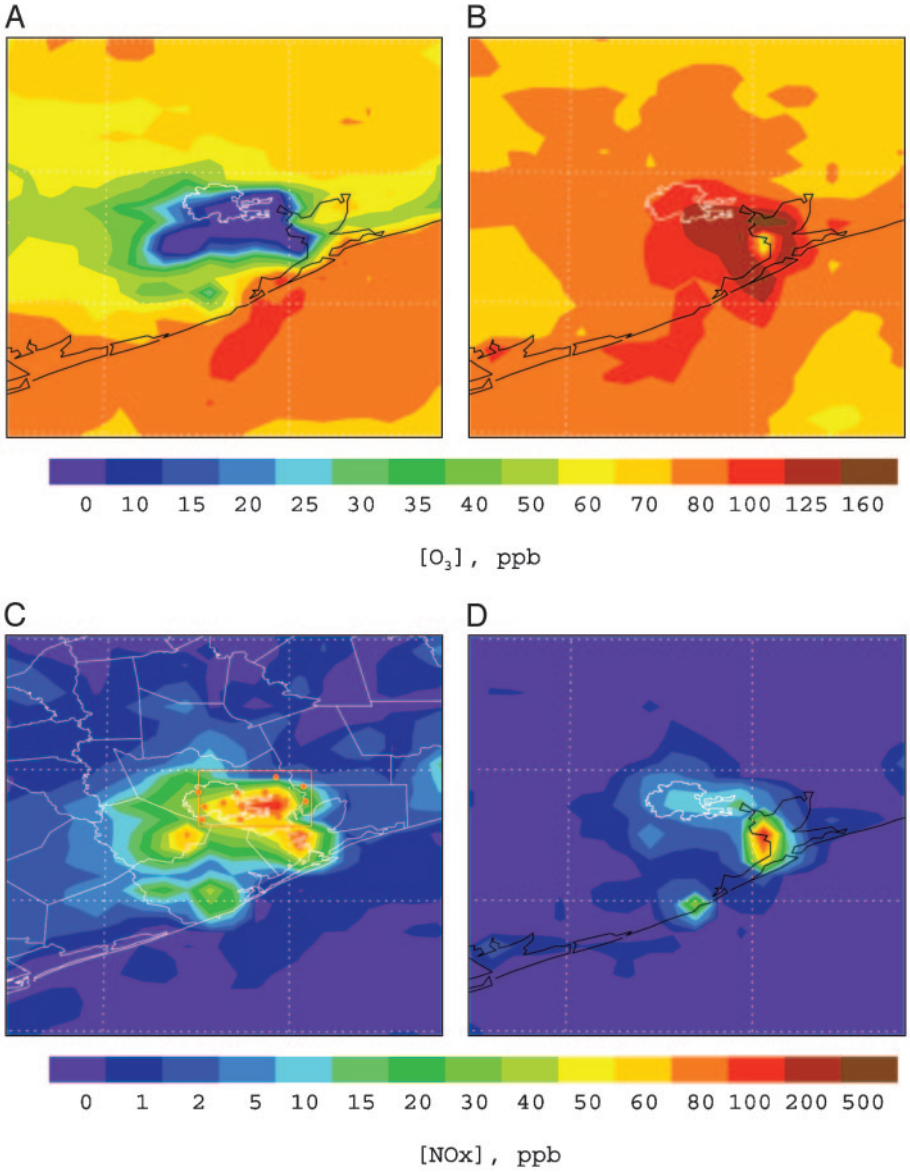

Fig. 2. Simulated surface O_3 (*A* and *B*) and NO_x (*C* and *D*) distributions at 11 p.m. (*A* and *C*) and 3 p.m. (*B* and *D*) CDT during the time period of September 7–8, 1993. The Houston City limit is marked by thin white lines, and the other white lines in *C* label the county limits near Houston. Also shown in *C* are the locations of surface air quality monitoring stations marked by the brown dots. The brown frame encompassing all of the stations is defined as the Houston domain in the text.

monitoring stations (15 for O_3 and 12 for NO_x, and 3 stations within the rectangle do not have NO_x data). The observation data are 1-h averaged values, whereas the model values are instantaneous. Also shown in Fig. 3*B* as the red dashed–dotted line (right vertical axis) is the NO_x emission rate averaged over the same domain. The two daily peaks of NO_x emission occurring around 6 a.m. and 4 p.m. CDT correspond to the morning and afternoon traffic peaks, respectively. The modeled temporal O_3 evolution confirms the drastic diurnal variation of surface ozone (Fig. 3*A*). The O_3 concentration rises rapidly after sunrise, reaches a peak in the early afternoon hours, and drops sharply after sunset, consistent with efficient photochemical ozone production during the daytime and rapid O_3 removal by NO at night. Similarly, the modeled NO_x evolution also exhibits a pronounced diurnal pattern (Fig. 3*B*). NO_x typically peaks before sunrise because of nighttime accumulation of industrially emitted NO and increasing automobile emission associated with the morning traffic. A NO_x minimum is maintained during the daytime hours because of vertical dilution and chemical processing, even if the NO_x emission remains high. Our modeled O_3 and NO_x diurnal variations are consistent with atmospheric measurements (Fig. 3). Throughout the episode, ozone is reasonably simulated, and the integral (time-averaged) agreement over the 5 days is within 10%. The model also captures the diurnal NO_x changes. The difference between the model and observation may be attributed to several factors, including the difference in the monitoring and model height and the horizontal and vertical resolutions of the model.

To quantify photochemical ozone formation, we computed the O_3 production rate as a function of NO_x concentration (Fig. 4). The chemical production rate of ozone is defined as $P(O_3) = d(O_x)/dt$, where $O_x = O(^1D) + O_3 + NO_2$. Note that during the daytime NO_2 can be reasonably assumed to achieve

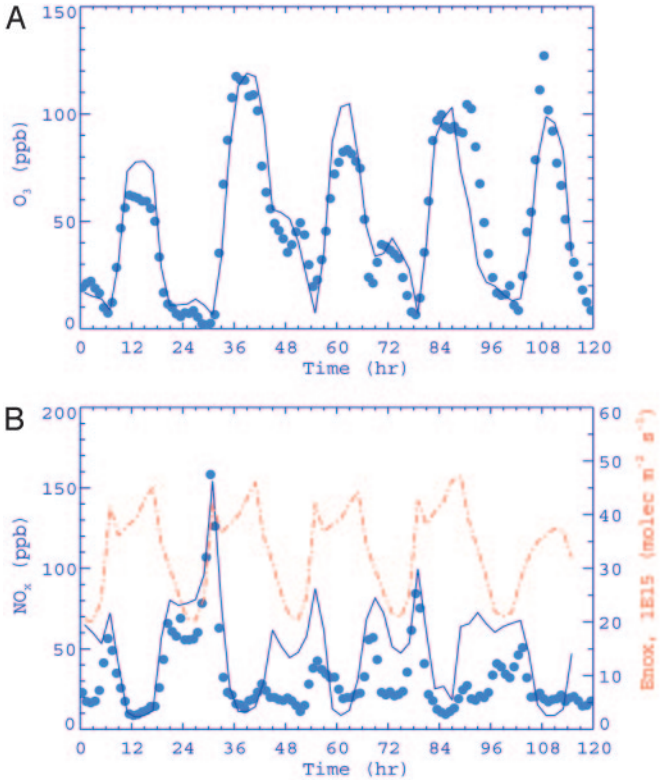

Fig. 3. Temporal evolution of simulated (solid lines) and observed (filled circles) surface O_3 (*A*) and NO_x (*B*) concentrations averaged over the Houston domain during September 7–11, 1993.

a steady state so that $d(O_x)/dt \approx d(O_3)/dt$. It is commonly believed that the O_3 production rate increases at low NO_x until a maximum is reached and then decreases at high NO_x (8, 13). This behavior occurs because high NO_x promotes removal of OH radicals by the OH reaction with NO_2 and hence reduces photochemical O_3 formation. In addition to NO_x, $P(O_3)$ is also dependent on VOC reactivity, sunlight, and radical precursors (8). Our calculations show that $P(O_3)$ does not exhibit the expected decrease at high NO_x and that the maximal O_3 production rate is not attained for the NO_x concentration as

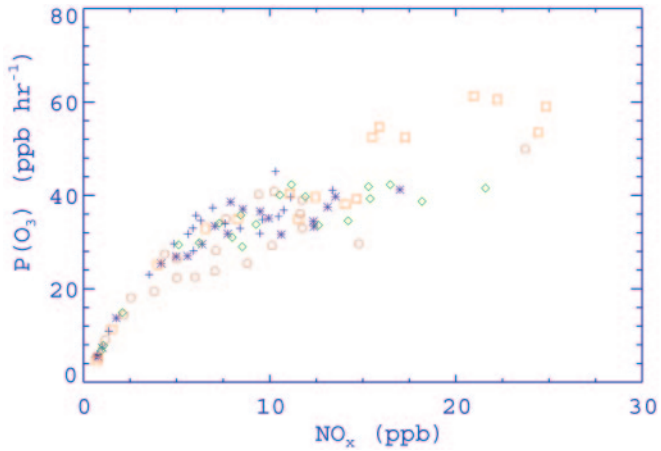

Fig. 4. Calculated O_3 production rate as a function of NO_x concentration at 3 p.m. CDT on the model grids within the Houston domain. The symbols represent the following simulation dates: +, 0907; *, 0908; ◇, 0909; □, 0910; ○, 0911.

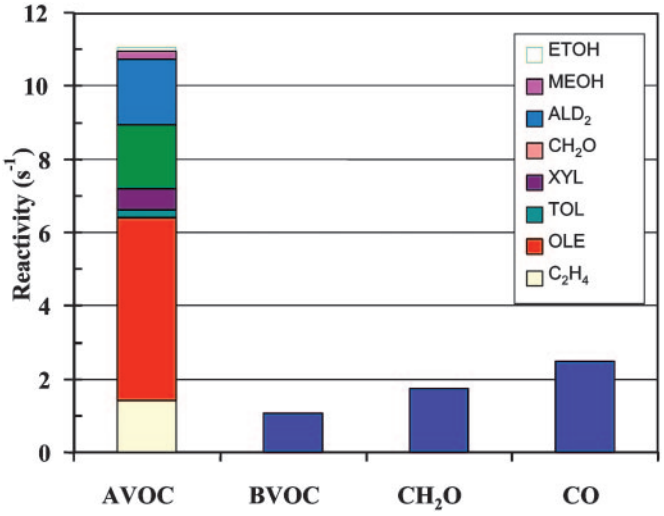

Fig. 5. Calculated VOC reactivity averaged over the entire episode within the bottom model layer in the Houston domain. AVOC, anthropogenic VOC; BVOC, biogenic VOC.

high as 20 ppbv. The O_3 production rates of >20 ppbv·h^{-1} prevail over much the Houston domain, and the largest $P(O_3)$ values (>40 ppbv·h^{-1}) occur exclusively in the industrial Houston Ship Channel region, both reflecting very high anthropogenic VOC reactivity. Our calculated O_3 production efficiency in the Houston metropolitan area is distinct from those found in other cities of the United States, such as Nashville, TN; New York; Philadelphia; and Phoenix (2, 5). Those cities have much less industrial emissions of VOCs and NO_x, with $P(O_3)$ being typically <20 ppbv·h^{-1}. Our results, however, are similar to another recent study that also shows high ozone production efficiency in heavily polluted industrial plumes over the Houston metropolitan area by analyzing aircraft data of VOCs, NO_x, and other ozone precursors measured during the recent Texas Air Quality Study (TexAQS 2000) (5).

The fact that the ozone production rate does not exhibit the expected decrease at high NO_x is explained by the very high VOC reactivity in this region that leads to abundant organic peroxy radicals (RO_2) to react with NO to produce O_3. The calculated VOC reactivity, defined as the product of the concentration of a VOC species and its rate constant with OH, is shown in Fig. 5. Anthropogenic VOCs (AVOCs) account for ≈50% of the total VOC reactivity, whereas biogenic VOCs (BVOCs) and CO account for 19% and 18%, respectively. Clearly, industrial VOCs such as alkenes (C_2H_4, OLE, and part of ALD2) dominate AVOCs in the O_3 production. Hence, the large abundance and high reactivity of AVOCs and the coexistence of abundant AVOCs and NO_x are responsible for the high O_3 production rates in this area.

Conclusions

Our model simulations reveal that ozone formation in the Houston metropolitan area is governed by complex interplay of chemical transformation, transport and mixing by meteorological circulation, and emissions from anthropogenic sources. The results show a striking pattern of the diurnal variation of surface ozone (O_3) in this region. During the daytime, photochemical oxidation of VOCs catalyzed by NO_x in the presence of sunlight results in episodes of high ambient O_3 levels of >200 ppbv, and at night an urban-scale surface ozone hole is formed. Our work unambiguously establishes the links between the rapid production, daily peak, and diurnal variation of surface O_3 and the

concurrence of high anthropogenic VOC and NO_x emissions. Regulatory control of industrial VOC and NO_x emissions, hence, will not only suppress the daytime O_3 peak but also will modulate the extreme diurnal variation of surface O_3 in this region.

We thank John Nielsen-Gammon (Texas A&M University) for assistance with the MM5 simulations, Jim Smith (Texas Commission on Environmental Quality) for providing the emission inventory data used in the simulations, and Robert A. Duce (Texas A&M University) for helpful comments on the manuscript. This work was supported by the Texas Air Research Center and the National Aeronautics and Space Administration New Investigator Program in Earth Science. The National Center for Atmospheric Research is supported by the National Science Foundation.

1. Chameides, W. L., Salyer, R. D. & Cowling, E. B. (1997) *Science* **276,** 916–916.
2. Ryerson, T. B., Trainer, M., Holloway, J. S., Parrish, D. D., Huey, L. G., Sueper, D. T., Frost, G. J., Donnelly, S. G., Schauffler, S., Atlas, E. L., *et al.* (2001) *Science* **292,** 719–723.
3. Thornton, J. A., Wooldridge, P. J., Cohen, R. C., Martinez, M., Harder, H., Brune, W. H., Williams, E. J., Roberts, J. M., Fehsenfeld, F. C. Hall, S. R., *et al.* (2002) *J. Geophys. Res.* **107,** 4146.
4. Chameides, W. L., Lindsay, R. W., Richardson, J. & Kiang, C. S. (1988) *Science* **241,** 1473–1475.
5. Kleinman, L. I., Daum, P. H., Imre, D., Lee, Y.-N., Nunnermacker, L. J., Weinstein-Lloyd, S. & Rudolph, J. (2002) *Geophys. Res. Lett.* **29,** 1467.
6. Carroll, R. J., Chen, R., George, E. I., Li, T. H., Newton, H. J., Schmiediche, H. & Wang, N. (1997) *J. Am. Stat. Assoc.* **438,** 392–404.
7. U.S. Environmental Protection Agency (1998) *National Air Quality and Emissions Trends Report 1998* (U.S. Environmental Protection Agency, Washington, DC), EPA 454/R-00-003.
8. Sillman, S., Logan, J. A. & Wofsy, S. C. (1990) *J. Geophys. Res.* **95,** 1837–1851.
9. Thompson, A. M. (1992) *Science* **256,** 1157–1165.
10. Zhang, R., Tie, X. & Bond, D. W. (2003) *Proc. Natl. Acad. Sci. USA* **100,** 1505–1509.
11. National Research Council (1991) *Rethinking the Ozone Problem in Urban and Regional Air Pollution* (Natl. Acad. Press, Washington, DC).
12. Hess, P. G., Flocke, S., Lamarque, J. F., Barth, M. C. & Madronich, S. (2000) *J. Geophys. Res.* **105,** 26809–26839.
13. Lei, W. (2003) Ph.D. dissertation (Texas A&M Univ., College Station).
14. Simonaitis, R., Meagher, J. F. & Bailey, E. M. (1997) *Atmos. Environ.* **31,** 27–43.
15. Zhang, R., Suh, I., Clinkenbeard, A. D., Lei, W. & North, S. W. (2000) *J. Geophys. Res.* **105,** 24627–24635.
16. Zhang, D., Zhang, R., Park, J. & North, S. W. (2002) *J. Am. Chem. Soc.* **124,** 9600–9605.
17. Ammann, M., Kalberer, M., Jost, D. T., Tobler, L., Rossler, E., Piguet, D., Gaggeler, H. W. & Baltensperger, U. (1998) *Nature* **395,** 157–160.
18. Kotamarthi, V. R., Gaffney, J. S., Marley, N. A. & Doskey, P. V. (2001) *Atmos. Environ.* **35,** 4489–4498.
19. Zhang, R., Leu, M. T. & Keyser, L. F. (1995) *Geophys. Res. Lett.* **22,** 1493–1496.
20. Brasseur, G. P., Hauglustaine, D. A., Walters, S., Rasch, P. J., Muller, J. F., Granier, C. & Tie, X. X. (1998) *J. Geophys. Res.* **103,** 28265–28289.
21. Grell, G. A. (1993) *A Description of the Fifth Generation Penn State/National Center for Atmospheric Research Mesoscale Model (MM5)*, *NCAR/TN-398+IA* (National Center for Atmospheric Research, Boulder, CO).
22. Orville, R. E., Huffines, G., Nielsen-Gammon, J., Zhang, R., Ely, B., Steiger, S., Philips, S., Allen, S. & Read, W. (2001) *Geophys. Res. Lett.* **28,** 2597–2600.
23. Lawson, D. R. (1995) *Coastal Oxidant Assessment for Southern Texas (COAST) Project: Final Report* (Texas Natural Resource Conservation Commission, Austin, TX).
24. Korc, M., Korc, M., Jones, C., Chinkin, L., Main, H. & Roberts, P. (1995) *Use of PAMS Data to Evaluate the Texas COAST Emission Inventory* (U.S. Environmental Protection Agency, Washington, DC).
25. Wesely, M. L. (1989) *Atmos. Environ.* **23,** 1293–1304.
26. Zhang, D. & Zhang, R. (2002) *J. Am. Chem. Soc.* **124,** 2692–2703.
27. Zhang, D., Lei, W. & Zhang, R. (2002) *Chem. Phys. Lett.* **358,** 171–179.